5th Joint International Symposium on Deformation Monitoring (JISDM), 20-22 June 2022, Valencia, Spain
DOI: http://doi.org/10.4995/JISDM2022.2022.13839

InSAR displacement time series post-processing to back-analyze a slope failure

Dora Roque[1], Martino Correia[2], Ricardo Cabral[2], Steffan Davies[2], Tiago Cordeiro[2], Ana Fonseca[1], Paulo Barreto[3]

[1] Laboratório Nacional de Engenharia Civil, Lisboa, Portugal, (droque@lnec.pt; anafonseca@lnec.pt)
[2] THEIA, Coimbra, Portugal, (hello@theia.pt)
[3] EGIS Road Operation Portugal, Lamego, Portugal, (paulo.barreto@egisportugal.pt)

Key words: *InSAR; time series post-processing; back-analysis; slope failure*

ABSTRACT

In this study, the failure of a slope adjacent to a motorway was back-analyzed based on InSAR data. The location of the slided area and the exact date of the event were not known in advance. A post-processing strategy was applied on the displacement time series in order to aid the detection of instability signs and to enable the identification of the location and the narrowing down of the time interval of the slide. InSAR displacement time series were obtained following the small baseline subset approach implemented on an automatic processing platform. Distributed scatterers were clustered based on the similarity of their displacement time series, in order to form clusters of scatterers with similar behavior. This procedure allowed the computation of displacement time series representative of each cluster, aiding the detection of instability signs on the slope. One of the clusters showed a sudden movement away from the SAR sensor. It was later confirmed that the slide had occurred at the location of the scatterers belonging to that cluster and during the time interval between the two observation epochs corresponding to the break in the time series. In conclusion, the proposed method was effective in the back-analysis of the slope failure, hopefully contributing to the uptake of InSAR technology by structural safety experts.

I. INTRODUCTION

Interferometric Synthetic Aperture Radar (InSAR) has proved to be an effective technology for the monitoring of deformation caused by earthquakes, volcanic eruptions, glacier movement, urban subsidence, landslides, among others (Crosetto *et al*., 2016). Some authors have also used InSAR to monitor civil infrastructures (*e.g.* Di Martire *et al*., 2014; Emadali *et al*., 2017; Giardina *et al*., 2019; Lazecky *et al*., 2017; Milillo *et al*., 2019), profiting from its spatial coverage and temporal resolution. However, its application in this field remains a challenging task, due to several factors:

1. Typical structure monitoring methods achieve higher accuracies;
2. Lack of redundant observations;
3. Displacements are measured along the SAR line-of-sight (LOS);
4. Observation frequency does not enable the monitoring of structure dynamic behavior;
5. Large volume of data may be difficult to interpret by InSAR non-experts.

The aforementioned reasons prevent the uptake of InSAR technology in the field of structural safety.

Typically, large volumes of data are achieved using InSAR, in which hundreds or even thousands of measurement points are obtained per square kilometer, each of them having displacement time series possibly with hundreds of observation epochs associated. The exploration of these results is a big data problem and turn the displacement interpretation difficult to perform by InSAR non-experts. In the particular case of structural behavior, which varies over time, variables typically analyzed in InSAR products, such as average velocity or cumulative displacement during a certain time interval, do not provide all the potential knowledge InSAR data contain for structure monitoring. Therefore, the development of automatic methods to extract information from the displacement time series is of the utmost importance in this field.

This study aims at contributing to increase the trust of structural safety experts in InSAR data by evaluating the capabilities of this technology to back-analyze movement on a slope affected by a landslide. A blind test was performed, in which the goal was to use InSAR data to identify the slope area affected by the landslide and to narrow down the time interval of its occurrence. InSAR displacements were computed through an automatic InSAR processing platform for a motorway and its surroundings, including the slope that is the study object of this paper. The InSAR displacement time series of the points located on the slope were evaluated through a semi-automatic procedure to form clusters of points with similar behavior. This aggregation of information allowed the detection of slope behavior patterns in space and time and enabled the attainment of the answers sought in the blind test. The applied

method is an improvement of that presented in Roque *et al*. (2018), by including a post-processing method to correct unwrapping errors and to analyze partial time series.

The paper is organized as follows. Section II presents the methods used in the study, with Subsection A describing the InSAR processing and Subsection B presenting the time series clustering. Section III contains a description of the area of interest (AOI) and of the SAR image dataset. Section IV shows the achieved results and is followed by their discussion in Section V. The paper is finished by the main conclusions of the study in Section VI.

II. Methods

A. *InSAR processing*

Displacements were computed from a stack of SAR images through an automatic InSAR processing platform. In order to prepare the dataset for multi-temporal analysis, GMTSAR was employed to corregister the products from the stack and generate interferograms using the SBAS model. A maximum temporal baseline was limited to 48 days, maximum spatial baseline was defined as 100 metres, and the threshold for acceptable amplitude dispersion was set to 0.6. The scene was divided into 4 patches, which was sufficient considering the relatively small area of interest.

GMTSAR results were properly structured in order to be recognised by the StaMPS/MTI software, where point processing was performed in order to extract subsidence values for the area of interest. No point weeding was undertaken. After processing, the data was inverted in order to convert from multi-master to single-master displacement estimation.

The points from StaMPS/MTI processing were exported in a tabular data format for post-processing compatible with the StaMPS-Visualizer application. Average velocity and displacement time series were achieved for each point.

B. *Time series clustering*

The goal of the post-processing of the InSAR data was the identification of spatiotemporal patterns in the behavior of the distributed scatterers, by clustering them according to the similarity between their displacement time series. The clustering algorithm was composed by several steps and was implemented in R software (R Core Team, 2021).

1) Input data: InSAR displacement time series were the only data required for the algorithm application, with a displacement observation for each SAR image acquisition date. Gaps in the acquisition were filled with interpolated values.

The displacement time series were complemented by auxiliary (and optional) information achieved in the InSAR processing, but also by external data provided as raster files. In this study, InSAR derived velocities and slope data were considered.

2) Removal of reference point effect: In case the point used as reference presented some movement, its displacements influenced the time series of all the other points. In this study, an adaptation of the method presented in Notti *et al*. (2015) was applied in order to remove this effect. The points presenting absolute value of average velocity lower or equal than 0.5 mm/year were considered to be stable and the average of their displacement time series, which corresponded to the effect of the reference point on the other points, was removed from the displacement time series of all points in the AOI.

3) Correction of unwrapping errors: Unwrapping errors were detected in the displacement time series and were corrected following Notti *et al*. (2015). Time series were searched for consecutive displacement values with absolute difference larger than ¼ of the SAR signal wavelength. In such cases, the second displacement value in the pair might be affected by an unwrapping error and became a candidate to a potential correction. However, the displacement value was corrected only if an external factor capable of causing a large displacement occurred at that date. Rainfall is an external factor that frequently works as a trigger to landslides. Therefore, daily rainfall data were collected from a meteorological station near the AOI for the same time interval of the displacement analysis. Dates were eligible for unwrapping error correction in case the amount of rainfall in that day was greater or equal than the 90% percentile of the daily rainfall in the whole time interval. The correction was applied on the displacement values if the displacement and rainfall conditions were both met for the same date. If the displacement value to be corrected was greater than that from the previous epoch, ½ of the SAR signal wavelength was subtracted to that displacement value. On the other hand, if the displacement value to correct was lower than the previous one, ½ of the SAR signal wavelength was added to it (Figure 1).

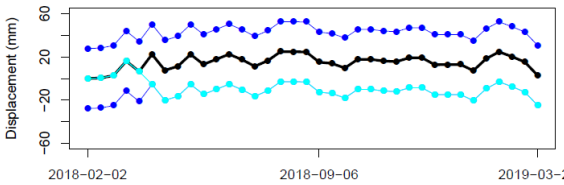

Figure 1. Displacement time series obtained during InSAR processing (black), displacement time series ±½ of the SAR signal wavelength (dark blue) and corrected displacement time series (cyan).

4) Time series cut: Previous studies have shown that the time series post-processing method was little sensitive to small magnitude changes in long time series (Roque, 2020).

In order to increase its sensitivity to signs of instability on the AOI around the time of the landslide, temporal subsets of the time series were considered. The removal of the reference point effect and the unwrapping error correction were performed on the complete displacement time series; however, they were later cut into a smaller time interval, narrowing down the analysis to the approximate date of the landslide occurrence (Section III).

5) Compute dissimilarity matrix: The clustering procedure was applied on the cut displacement time series. A hierarchical agglomerative clustering was used. In the first step, each point was considered as an individual cluster. The similarities between each pair of groups were computed and the most similar ones were merged. This procedure was performed iteratively until all clusters were aggregated into a single one. The similarities were the distances between the displacement time series, which were determined through the Dynamic Time Warping (DTW) method (Berndt and Clifford, 1994). DTW distance between two time series corresponds to the minimum cumulative path among several possibilities of connecting the data points (displacement observations in this case) from both series (Figure 2). Connections are not required to be between data points from the same epochs.

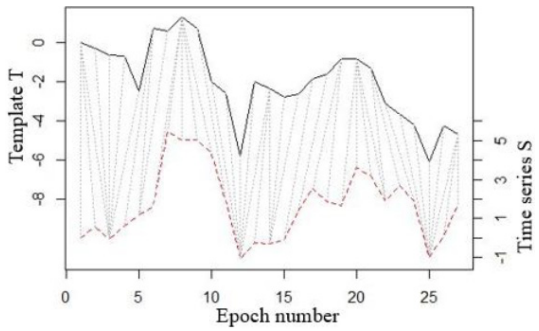

Figure 2. Connections between the data points from the template time series T and a generic time series S.

The aggregation method used in the clustering was the complete linkage, which considers the farthest elements in a pair of clusters to determine the distance between the two groups, *i.e.*, in this study, the distance between a pair of clusters was calculated as the DTW distance between the most dissimilar displacement time series from both groups. This method formed homogeneous clusters and was sensitive to the presence of outliers. The distances between each pair of clusters, in each iteration, were organized in a dissimilarity matrix, which provided the information for the cluster formation.

6) Selection of the number of clusters: For each iteration, the pair of clusters presenting the smallest value in the dissimilarity matrix was merged. The distance between two merged clusters is called linkage distance.

The analysis of linkage distances from all iterations assisted the selection of the number of clusters to be considered for analysis. The largest values were observed at the last iterations (top of the chart in Figure 3), when the merged clusters were already distinct. The number of clusters to analyze was selected in order to assure that the linkage distances connecting the elements inside each group were low. This procedure led to the construction of clusters formed by points with similar displacement time series. It also assured the clusters had different behavior among each other.

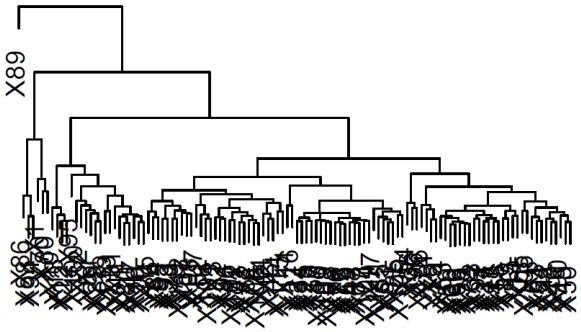

Figure 3. Chart of linkage distances (vertical black lines); the alphanumeric codes at the bottom of the chart correspond to the individual clusters in the first step.

After the cluster formation, data for their interpretation were computed. The displacement time series representative of the behavior of each cluster were achieved by averaging the displacement time series of all points in each group. Furthermore, the values of the auxiliary variables were used to compute cluster centroids. Velocities were already associated to the points during the InSAR processing, while slope values from the raster file were attributed to each point according to their location. The values from both variables were averaged for each cluster.

III. Study Area and Dataset

The AOI for this study was a slope adjacent to a motorway, in Portugal. It was located at a granite area and it was built in the 2000 s. The slope occupies an area of approximately 10000 m^2, it faces east and its average slope is 15° (Figure 4).

For the blind test performed in this study, it was known in advance that a landslide occurred on part of the slope during March 2019. In order to identify the affected area and to narrow down the time interval of the event, InSAR displacements were computed through the InSAR processing platform from Section II A and then evaluated through the time series post-processing method from Section II B.

The SAR dataset was composed of 33 Sentinel-1 A SLC (Single Look Complex) products in IW (Interferometric Wide) swath mode, using a descending orbit, starting on 2nd of February 2018 and ending on the 29th of March 2019, with a minimum interval of 12 days. The orbit path and frame of these products was 52 and 458,

respectively. ESA's SNAP (Sentinel Application Platform) software was used to determine the ideal master product from the stack, based on satellite baselines and dates, which was the product corresponding to the 18th of September 2018.

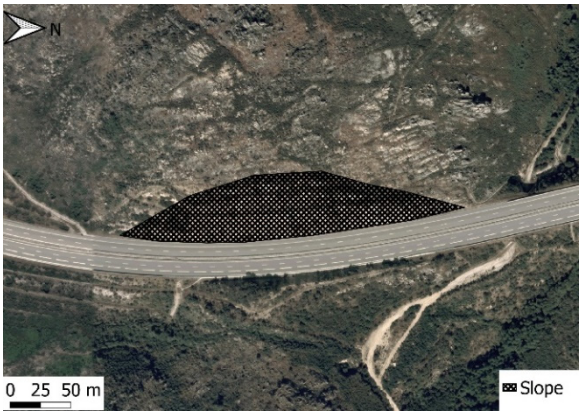

Figure 4. Slope adjacent to motorway.

At the post-processing analysis, the time series were cut to the time interval between January and March 2019 to increase the algorithm sensitivity to the displacements occurred in March 2019 (Section II B 4).

IV. Results

A. *InSAR processing*

The InSAR processing led to 116 points on the slope, with average velocities between 22.3 mm/year away from the sensor and 11.3 mm/year towards it, from February 2018 to March 2019 (Figure 5).

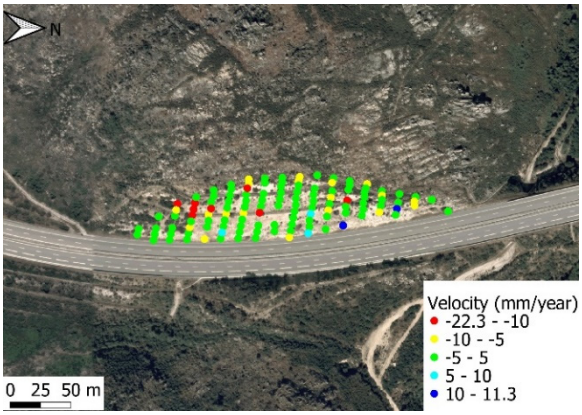

Figure 5. Velocity map for the points on the slope.

The velocity map presented several points with average velocities away from the sensor above 10 mm/year at the southernmost area of the slope. However, there were other areas with similar velocity values. Furthermore, there were also points presenting velocities towards the sensor with magnitudes of centimeters per year, which might correspond to horizontal displacement from west to east, *i.e.*, towards the motorway.

B. *Time series clustering*

The analysis of the linkage distance chart from Figure 3 led to the organization of the points into seven clusters, with a varying number of elements (Table 1).

Table 1. Point distribution throughout the clusters

Cluster	Points	
	Number	Percentage (%)
1	3	2.6
2	54	46.6
3	35	30.2
4	16	13.8
5	4	3.4
6	3	2.6
7	1	0.9

Figure 6 presents the spatial distribution of the points throughout the clusters. Some of the groups were spatially cohesive (cluster 5 and most of clusters 4 and 6), while the others were spread throughout the slope. Cluster 7 was formed by a single point, meaning it was the point identified in Figure 3 with the alphanumeric code X89. The chart shows this point had a displacement time series distinct from those of the remaining ones, as this was the last point being aggregated to the main cluster.

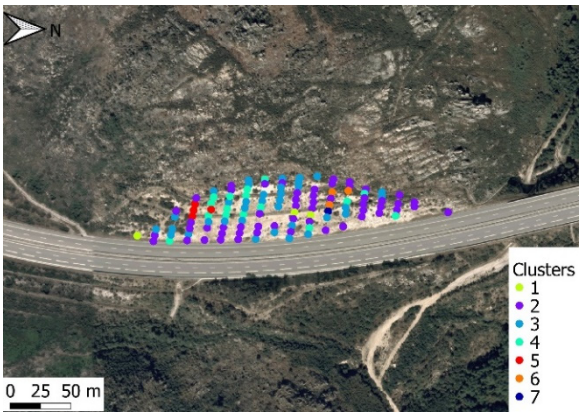

Figure 6. Cluster spatial distribution.

Displacement time series representative of each cluster behavior were determined for each group and they are presented in Figure 7. During the first three months of 2019, average displacements varied between 20 mm away from the sensor and 15 mm towards it.

The centroids for velocity and slope were computed for each cluster and are presented in Figures 8 and 9, respectively. Although the clusters were built based on the displacement time series between January and March 2019, in order to increase the chances of isolating the area affected by the landslide in a single cluster, the velocity values in the chart correspond to the complete time interval of the analysis (February 2018 – March 2019) to capture possible early signs of instability.

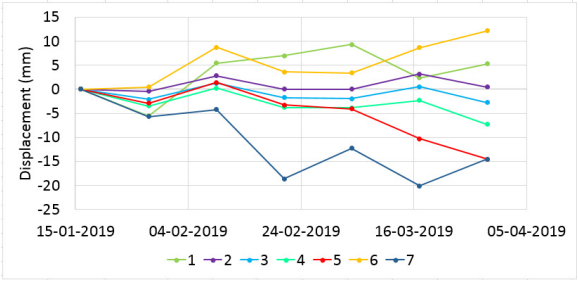

Figure 7. Displacement time series representative of cluster behavior.

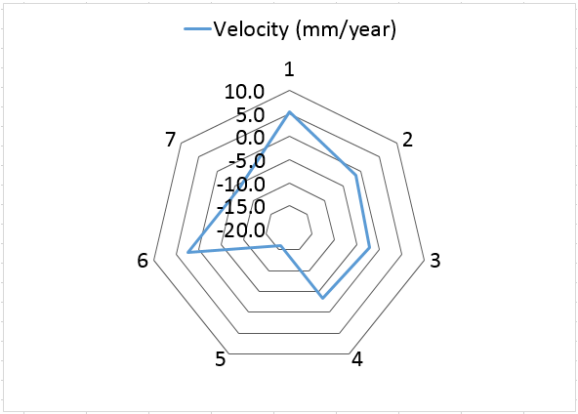

Figure 8. Centroids for velocity between February 2018 and March 2019.

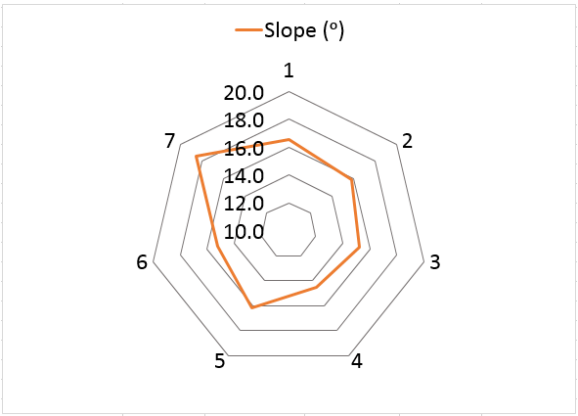

Figure 9. Centroids for slope.

From Figure 8, it was verified that cluster 5 presented the largest average velocity away from the sensor (more than 15 mm/year) and was followed by cluster 7, with average velocity around 5 mm/year. On the other hand, clusters 1 and 6 moved towards the sensor during the 14 months of the analysis. Clusters 2, 3 and 4 had average velocities close to 0 mm/year. Slope centroids in Figure 9 show that cluster 7 was the one located on the steepest slope region, followed by clusters 1 and 5. The three clusters all had average slope above 16°. Clusters 2, 3, 4 and 6 had slightly lower slopes, but still large enough for these areas to be susceptible to landslide occurrence.

V. Discussion

The results presented in the previous section were analyzed in order to achieve the answers required for the blind test. The velocity map showed several points with velocities above 10 mm/year between February 2018 and March 2019, either away from the sensor or towards it. On one hand, movement away from the sensor might correspond to settlement and could be a sign of slope instability. There were a few points with movement away from the sensor at the southernmost part of the slope forming a spatially cohesive group, which suggested the landslide might have occurred on that area. However, there were points on other areas of the slope with similar behavior. On the other hand, some points presented movement towards the sensor, which might also correspond to slope instability, as they were compatible to horizontal movement towards the motorway. Therefore, the analysis of the displacement time series was required to identify univocally the affected area.

Seven distinct behavior patterns were identified on the slope through the clustering of the displacement time series. Clusters 2, 3 and 4 presented similar behavior, with the displacement time series showing identical trends. Together, the three clusters contained 90.6% of the points on the slope. The representative displacement time series presented oscillations around 0 mm, suggesting the three clusters mostly had a stable behavior from January to March 2019 and their movement could be considered as the expected behavior of the slope. The remaining clusters (1, 5, 6 and 7) presented behavior distinct from the expected one, which might correspond to signs of instability (Figure 10). The analysis of velocity centroids from Figure 8 for clusters 1, 5, 6 and 7 revealed that cluster 5 was the one with the largest velocity between February 2018 and March 2019 (above 15 mm/year away from the sensor), *i.e.*, the points in this cluster were already moving for several months before the landslide in March 2019. The slope centroids from Figure 9 showed all clusters were subjected to similar slope conditions; however, cluster 5 was located on one of the steepest areas of the slope, which might have contributed to increase the landslide susceptibility in the area. The aforementioned analysis suggested that the points forming cluster 5 were the most likely to be located on the area affected by the landslide.

Analyzing the displacement time series representative of the behavior of cluster 5 (Figure 7), it was observed that it was very similar to that of cluster 4, following the expected behavior of the slope, until the 5th observation epoch (5th of March 2019). After this date, the points in cluster 5 began to move away from the sensor with a displacement rate of 159 mm/year. This behavior was in accordance with the hypothesis that cluster 5 might be the one corresponding to the affected area. Furthermore, the representative displacement time series suggested that the landslide might have occurred between the 5th and the 6th observation epochs (5th of March and 17th of March, respectively), when the change in the cluster behavior was verified. Indeed, after the performed

analysis, the structural safety experts revealed the landslide occurred at the southernmost area of the slope (the location of cluster 5) on the 5th of March.

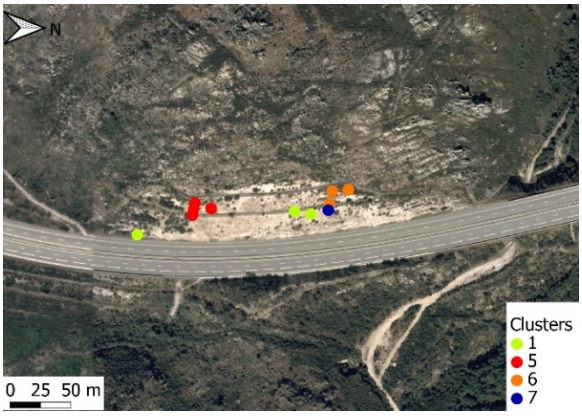

Figure 10. Spatial distribution of clusters potentially corresponding to slope instability areas.

Besides the correct identification of the landslide area, the performed analysis identified other areas of the slope presenting displacements deviating from the expected behavior (clusters 1, 6 and 7). These areas should keep being monitored through InSAR or in situ techniques, to detect eventual signs of instability in the future.

VI. Conclusions

This study intended to contribute to the uptake of InSAR technology by structural safety experts. The blind test was performed with the goal of verifying the capability of InSAR displacements to provide information about the slope behavior in the months before the landslide and the identifications of the affected area and of the approximate date of the event.

InSAR technology allowed a large spatial coverage of the slope, with a small number of gaps without observations. The usage of archived images enabled the analysis of the slope behavior in the year before the landslide occurrence. InSAR data alone enabled the identification of a few areas on the slope showing signs of potential instability. However, only the post-processing analysis of the displacement time series enabled the correct identification of the wanted answers. This strategy allowed the reduction of the data dimensionality into a small number of clusters, facilitating the detection of patterns in the points in both space and time. This led to the identification of deviations from the structure expected behavior, which can be used as early warning signs and trigger other monitoring activities, for example through in situ techniques.

In conclusion, InSAR data is capable of providing valuable knowledge on structural safety, especially when complemented with post-processing strategies.

VII. Acknowledgements

The authors would like to thank the Astropreneurs – Space Start-up Accelerator Programme for funding this study. Sentinel-1 data were provided by the European Space Agency. The orthophotographs were provided by the Portuguese Directorate-General for the Territory through the National Geographic Information System.

References

Berndt, D., and J. Clifford, (1994). Using dynamic time warping to find patterns in time series. In: *Workshop on Knowledge Discovery in Databases*, Seattle, Washington, July, pp. 359-370.

Crosetto, M., O. Monserrat, M. Cuevas-González., N. Devanthéry, and B. Crippa, (2016). Persistent Scatterer Interferometry: A review. *ISPRS Journal of Photogrammetry and Remote Sensing*, Vol 115, pp. 78-89.

Di Martire, D., R. Iglesias, D. Monells, G. Centolanza, S.Sica, M. Ramondini, L. Pagano, J.J. Mallorquí, and D. Calcaterra, (2014). Comparison between differential SAR interferometry and ground measurements data in the displacement monitoring of the earth-dam of Conza della Campania (Italy). *Remote Sensing of Environment*, Vol 148, pp. 58-69.

Emadali, L., M. Motagh, and M.H. Haghighi, (2017). Characterizing post-construction settlement of the Masjed-Soleyman embankment dam, Southwest Iran, using terraSAR-X SpotLight radar imagery. *Engineering Structures*, Vol 143, pp. 261-273.

Giardina, G., P. Milillo, M.J. DeJong, D. Perissin, and G. Milillo, (2019). Evaluation of InSAR monitoring data for post-tunneling settlement damage assessment. *Structural Control and Health Monitoring*, Vol 26, No. 2, p. e2285.

Lazecky, M., I. Hlavacova, M. Bakon, J.J. Sousa, D. Perissin, and G. Patrício, (2017). Bridge displacements monitoring using space-borne X-band SAR interferometry. *IEEE Journal of Selected Topics in Applied Earth Observations and Remote Sensing*, Vol 10, No. 1, pp. 205-210.

Milillo, P., G. Giardina, D. Perissin, G. Milillo, A. Coletta, and C. Terranova, (2019). Pre-collapse space geodetic observations of critical infrastructure: The Morandi Bridge, Genoa, Italy. *Remote Sensing*, Vol 11, No. 12, p. 1403.

Notti, D., F. Calò, F. Cigna, M. Manunta, G. Herrera, M. Berti, C. Meisina, D. Tapete, and F. Zucca, (2015). A user-oriented methodology for DInSAR time series analysis and interpretation: Landslides and subsidence case studies. *Pure and Applied Geophysics*, Vol 172, No. 11, pp. 3081-3105.

R Core Team, (2021). R: A language and environment for statistical computing. R Foundation for Statistical Computing, Vienna, Austria. URL: https://www.R-project.org/

Roque, D., (2020). Displacement measurement through InSAR geodesy for structural health monitoring. PhD thesis, Instituto Superior Técnico da Universidade de Lisboa, Lisboa, Portugal.

Roque, D., D. Perissin, A.P. Falcão, C. Amado, J.V. Lemos, and A.M. Fonseca, (2018). Analysis of InSAR displacements for the slopes around Odelouca reservoir. *Procedia Computer Science*, Vol 138, pp. 338-345.